

Exact calculation of Fourier series in nonconforming spectral-element methods

Aimé Fournier

NCAR Institute for Mathematics Applied to Geosciences

Boulder CO 80307-3000 USA

Key words: adaptive mesh refinement, Fourier analysis, spectral-element method

PACS: 02.30.Nw, 02.60.Cb, 02.60.Jh, 02.70.Dh, 02.70.Jn

1 Usefulness of calculating Fourier series in the SEM

In this note is presented a method, given nodal values on multidimensional nonconforming spectral elements, for calculating global Fourier-series coefficients. This method is “exact” in that given the approximation inherent in the spectral-element method (SEM), no further approximation is introduced that exceeds computer round-off error. The method is very useful when the SEM has yielded an adaptive-mesh representation of a spatial function whose global Fourier spectrum must be examined, e.g., in dynamically adaptive fluid-dynamics simulations such as [7].

Email address: fournier@ucar.edu (Aimé Fournier).

URL: <http://www.asp.ucar.edu/gtp/fournier> (Aimé Fournier).

2 Derivation of an exact transform

Suppose we have some functional problem in a spatial domain $\mathbb{D} := [-\pi, \pi]^d$ (possibly including toroidal geometry) and use coordinate transformations

$$\vec{\vartheta}_k \quad \text{from} \quad \vec{\xi} \in \mathbb{E}_0 := [-1, 1]^d \quad \text{to} \quad \vec{x} \in \mathbb{E}_k \quad (1)$$

to partition $\mathbb{D} = \bigcup_{k=1}^K \mathbb{E}_k$ by K elements $\mathbb{E}_k := \vec{\vartheta}_k(\mathbb{E}_0)$ with disjoint¹ interiors. Typically the SEM approximates the exact solution by its piecewise polynomial representation of degree P :

$$u^{\text{ex}}(\vec{x}) \approx u(\vec{x}) = \sum_{k=1}^K \sum_{\vec{j} \in \mathbb{J}} u_{\vec{j},k} \phi_{\vec{j},k}(\vec{x}), \quad (2)$$

where $\mathbb{J} := \{0, \dots, P\}^d$ indexes the values $u_{\vec{j},k} := u(\vec{x}_{\vec{j},k})$ and nodes $\vec{x}_{\vec{j},k} := \vec{\vartheta}_k(\vec{\xi}_{\vec{j}})$ mapped from the d -dimensional Gauss-Lobatto-Legendre (GLL) quadrature nodes $\xi_{\vec{j}}^\alpha := \xi_{j^\alpha} \in [-1, 1]$,

$$\phi_{\vec{j},k}(\vec{x}) := \begin{cases} \phi_{\vec{j}} \circ \vec{\vartheta}_k^{-1}(\vec{x}), & \vec{x} \in \mathbb{E}_k \\ 0, & \vec{x} \notin \mathbb{E}_k \end{cases} \quad (3)$$

is the $\vec{x}_{\vec{j},k}$ -interpolating piecewise-polynomial,

$$\phi_{\vec{j}}(\vec{\xi}) := \prod_{\alpha=1}^d \phi_{j^\alpha}(\xi^\alpha) \quad \text{and} \quad \check{\phi}_j(\xi) := \sum_{p=0}^P \check{\phi}_{j,p} L_p(\xi) \quad (4)$$

are $\vec{\xi}_{\vec{j}}$ - and ξ_j -interpolating polynomials, $\check{\phi}_{j,p} \equiv w_j L_p(\xi_j) / \sum_{j'=0}^P w_{j'} L_p(\xi_{j'})^2$ is a Legendre coefficient [e.g., 4, (B.3.15)], $\sqrt{p + \frac{1}{2}} L_p(\xi)$ is the orthonormal Legendre polynomial of degree p on $[-1, 1]$ and w_j is the GLL quadrature weight. In many cases a physically interesting quantity is the global Fourier-series coefficient $\hat{u}_{\vec{q}}$ at integer wavenumber components q^α , usually approximated by

¹ $\mathbb{E}_k \cap \mathbb{E}_{k'} = \emptyset$ if $k \neq k'$

M^d -point trigonometric d -cubature in such manner as

$$\hat{u}_{\vec{q}} := \frac{1}{(2\pi)^d} \int_{\mathbb{D}} u(\vec{x}) e^{-i\vec{q}\cdot\vec{x}} dv(\vec{x}) \equiv \sum_{k=1}^K \sum_{\vec{j} \in \mathbb{J}} \hat{\phi}_{\vec{j},k,\vec{q}} u_{\vec{j},k}, \quad (5)$$

$$\text{where } \hat{\phi}_{\vec{j},k,\vec{q}} = \frac{1}{M^d} \sum_{\vec{m} \in \mathbb{M}} \phi_{\vec{j},k}(\vec{x}_{\vec{m}}) e^{-i\vec{q}\cdot\vec{x}_{\vec{m}}} - \mathcal{E}_{\vec{q}} \phi_{\vec{j},k}, \quad (6)$$

$dv(\vec{x}) := \prod_{\alpha=1}^d dx^\alpha$ is the volume differential and $\mathbb{M} := \{1, \dots, M\}^d$ indexes trigonometric nodes $x_{\vec{m}}^\alpha := (2m^\alpha/M - 1)\pi$. Note whenever \mathbb{D} is adaptively repartitioned there is an additional computation cost of $\mathcal{O}(M^d)$ per node to use (2) to provide in (6) the values $\phi_{\vec{j},k}(\vec{x}_{\vec{m}})$, as well as a d -cubature error [generalizing 3, theorem 4.7]

$$\mathcal{E}_{\vec{q}} u \equiv \sum_{\vec{r} \in \mathbb{Z}^d \setminus \{\vec{0}\}} \hat{u}_{\vec{q}+M\vec{r}}$$

that in general converges no faster than $\mathcal{O}(M^{-2})$, because \mathbb{C}^1 discontinuities of (2) across element boundaries cause $|\hat{u}_{\vec{q}}|$ to decay only as $\mathcal{O}(|\vec{q}|^{-2})$. We discover a more accurate method by substituting (3) into (5) to yield

$$\begin{aligned} \hat{\phi}_{\vec{j},k,\vec{q}} &= \frac{1}{(2\pi)^d} \int_{\mathbb{E}_k} e^{-i\vec{q}\cdot\vec{x}} \phi_{\vec{j}} \circ \vec{\vartheta}_k^{-1}(\vec{x}) dv(\vec{x}) \\ &\stackrel{(1)}{=} \frac{1}{(2\pi)^d} \int_{\mathbb{E}_0} e^{-i\vec{q}\cdot\vec{\vartheta}_k(\vec{\xi})} \phi_{\vec{j}}(\vec{\xi}) \left| \frac{\partial \vec{\vartheta}_k}{\partial \vec{\xi}} \right| dv(\vec{\xi}) \\ &\stackrel{(4)}{=} \frac{1}{(2\pi)^d} \int_{\mathbb{E}_0} e^{-i\vec{q}\cdot\vec{\vartheta}_k(\vec{\xi})} \left(\prod_{\alpha=1}^d \sum_{p=0}^P \check{\phi}_{j^\alpha,p} L_p(\xi^\alpha) \right) \left| \frac{\partial \vec{\vartheta}_k}{\partial \vec{\xi}} \right| dv(\vec{\xi}). \end{aligned}$$

In many applications, especially when u -structure rather than domain geometry is guiding the mesh adaption, each \mathbb{E}_k is a d -parallelepiped with center \vec{a}_k and d legs $2\vec{h}_k^\alpha$, so we have an affinity $\vec{\vartheta}_k(\vec{\xi}) := \vec{a}_k + \vec{h}_k \cdot \vec{\xi}$, where \vec{h}_k^α make up the columns of \vec{h}_k . Then we obtain

$$\hat{\phi}_{\vec{j},k,\vec{q}} = \frac{1}{(2\pi)^d} \left| \vec{h}_k \right| e^{-i\vec{q}\cdot\vec{a}_k} \prod_{\alpha=1}^d \sum_{p=0}^P \check{\phi}_{j^\alpha,p} \int_{-1}^1 e^{-i\vec{q}\cdot\vec{h}_k^\alpha \xi} L_p(\xi) d\xi.$$

Finally, recalling the classical identity [e.g., 1, exercise 12.4.9] for the spherical Bessel function $B_p(r)$ of the first kind,

$$B_p(r) \equiv \frac{i^p}{2} \int_{-1}^1 e^{-ir\xi} L_p(\xi) d\xi, \quad (7)$$

$$\text{we obtain } \hat{\phi}_{\vec{j},k,\vec{q}} = \frac{1}{\pi^d} \left| \vec{h}_k \right| e^{-i\vec{q}\cdot\vec{a}_k} \prod_{\alpha=1}^d \sum_{p=0}^P \check{\phi}_{j^\alpha,p} i^{-p} B_p(\vec{q} \cdot \vec{h}_k^\alpha). \quad (8)$$

Note that most expressions in (8) can be precomputed; objects that may vary during a dynamically adaptive computation, such as \vec{a}_k or \vec{h}_k^α , typically take values from a sparse set, e.g., a collection of powers of 2. The computation of (5) now incurs no additional error beyond that of (2). Also note, to generalize to the case $P = P_k^\alpha$ is straightforward.

3 Accuracy of transform for 1D & 2D test cases

Equation (8) was implemented in MatLab[®] and tested using known results for (5). The most immediate test follows from (7), namely $\hat{u}_q^{\text{ex}} = \widehat{L_p(\cdot/\pi)}_q = i^{-p} B_p(\pi q)$. In this case (5) was found to reproduce (7) to 12-16 digits for $K = 1$, $P \leq 18$, implying similar performance for any polynomial $u(\vec{x})$ in this range. The next test was to put $u^{\text{ex}}(x) = \sin x$, or $\hat{u}_q^{\text{ex}} = (\delta_{q,1} - \delta_{q,-1})/2i$. Since this is not a polynomial we should expect at best to see algebraic convergence w.r.t. K in a uniform meshing $a_k = (k-1)h_k - \pi$, $h_k = 2\pi/K$ and exponential convergence w.r.t. P , as verified in Fig. 1. Note there is no need to test $u^{\text{ex}}(x) = \sin rx$ for $r > 1$ because of scaling.

We conclude by examining three 2D tests with adaptive meshing in the fashion of [5], using MatLab[®]. Fig. 2 confirms (5) in the case [6, (19)]

$$u^{\text{ex}}(\vec{x}) \equiv \sum_{\vec{q} \in \mathbb{Z}^2} e^{b^1|q^1| + b^2|q^2| + i\vec{q}\cdot\vec{l}\cdot\vec{x}}, \quad (9)$$

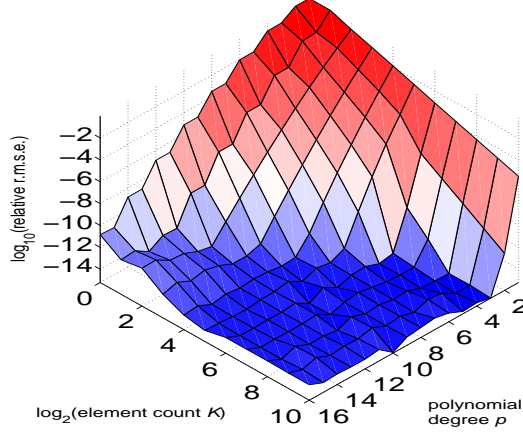


Fig. 1. Surface plot (blue low to red high) of \log_{10} relative r.m.s. error in (5) for $u^{\text{ex}}(x) = \sin x$, vs $\log_2 K$ and P .

where $b^\alpha = -\frac{2}{5}$ and $\vec{l} \doteq \begin{pmatrix} l^1 & l^2 \\ -l^2 & l^1 \end{pmatrix} = \begin{pmatrix} -\frac{1}{2} & 2 \\ 2 & 1 \end{pmatrix}$ is a biperiodicity-preserving “rotation”. As expected, the red curve (connecting the $|\hat{u}_{\vec{q}}|$ peaks) shows a power-law decay in \vec{q} -space. Note, in this plot and those below the \vec{l} -operation helps instigate mesh adaption but has the consequence of leaving \vec{q} undersampled in \mathbb{Z}^2 . In Fig. 3 is shown an initial condition [6, (22)]

$$\vec{u}^{\text{ex}}(0, \vec{x}) := -\vec{l} \sin \vec{l} \cdot \vec{x} \quad (10)$$

for the 2D Burgers eq. As expected, $\hat{u}_{\vec{q}}$ almost vanishes for $\vec{q} \neq \pm \vec{l}$. Finally, at time $t = 1.6037/\pi|\vec{l}|^2$ the analytic solution generalizing [2, (2.5)] to 2D is shown in Fig. 4. As expected for the *nearly* \mathbb{C}^0 -discontinuous fronts $\perp \vec{l}$ seen at left, $|\hat{u}_{\vec{q}}^1|$ decays slightly faster than $\mathcal{O}(|\vec{q}|^{-1})$ but *only for wavevectors* $\vec{q} \parallel \vec{l}$ (red curve).

References

- [1] George Arfken, 1985: *Mathematical methods for physicists*, 3rd ed., Academic Press, 985 pp.

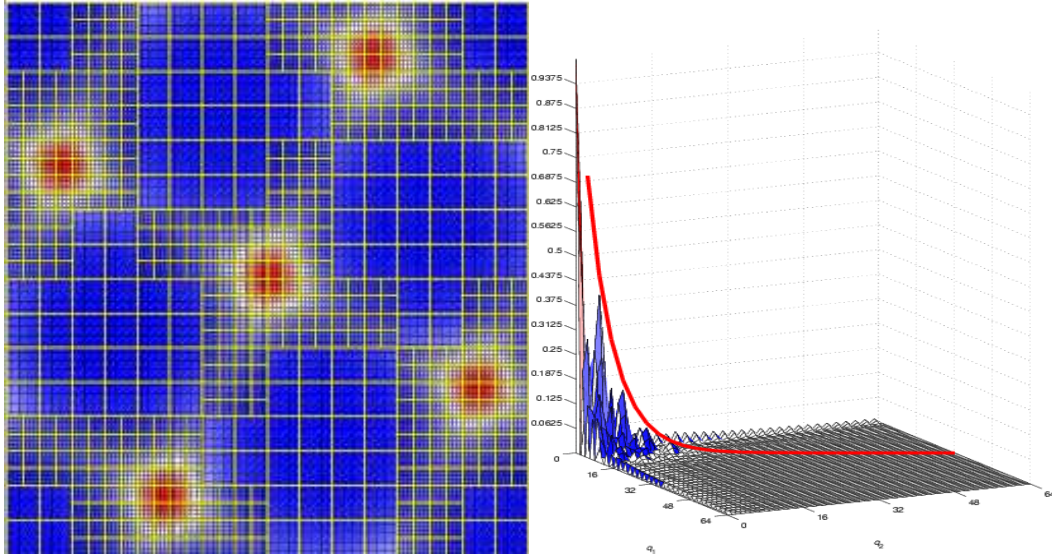


Fig. 2. Left, $u(9)$ over the spatial \vec{x} domain, increasing from blue to red; yellow lines indicate element boundaries, black lines show nodes $\vec{x}_{j,k}$ with $P = 5$. Right, surface plot of $|\hat{u}_{\vec{q}}|$ from (5) vs q^1 and q^2 .

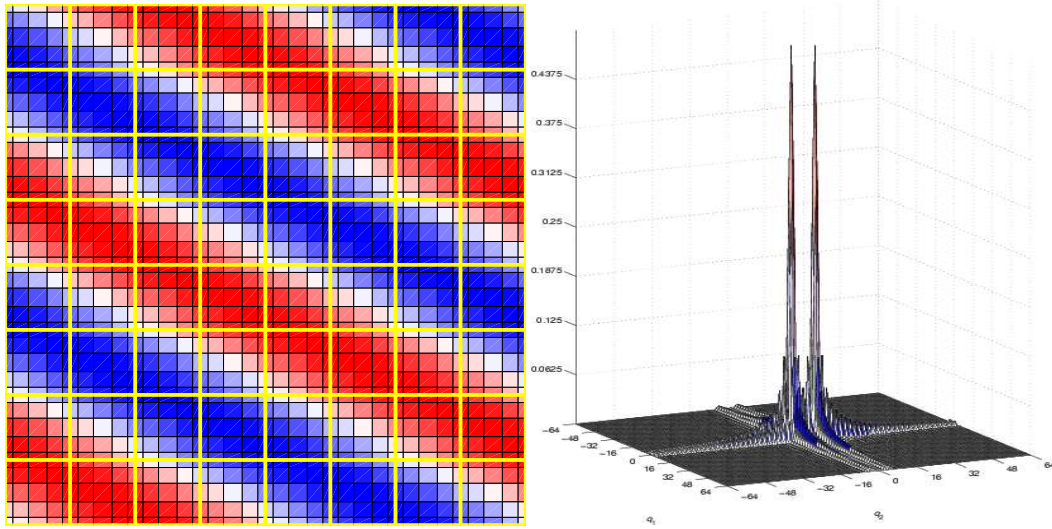


Fig. 3. As in Fig. 2 but for the $t = 0$ state given by (10), in $K = 2^6$ elements.

[2] C. Basdevant, M. Deville, P. Haldenwang, J.M. Lacroix, J. Ouazzani, R. Peyret & P. Orlandi, 1986: Spectral and finite difference solutions of the Burgers equation. *Computers & Fluids*, **14**, 23–41.

[3] John P. Boyd, 1989: *Chebyshev & Fourier spectral methods*, Springer, 793 pp.

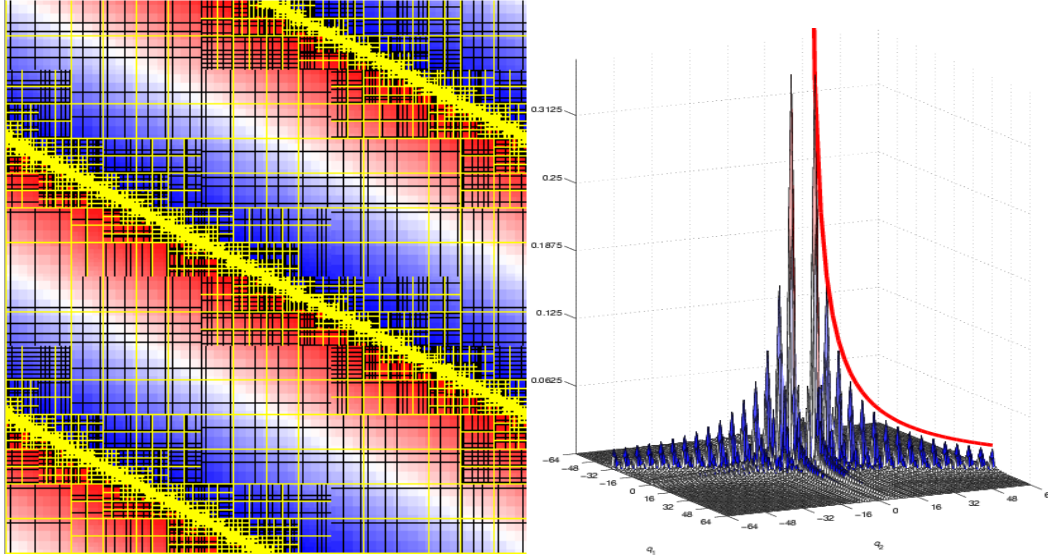


Fig. 4. As in Fig. 3 but for $t = 1.6037/5\pi$.

- [4] M.O. Deville, P.F. Fischer & E.H. Mund, 2002: *High-order methods for incompressible fluid flow*, Cambridge, 499 pp.
- [5] A. Fournier and D. Rosenberg, 2005: “Multiresolution adaptive spectral-element modeling of geophysical fluid dynamics using GASpAR,” in preparation.
- [6] Fournier, A., G. Beylkin and V. Cheruvu, 2005: Multiresolution adaptive space refinement in geophysical fluid dynamics simulation. *Lecture Notes Comp. Sci. Eng.*, **41**, 161–170.
- [7] Rosenberg, D., A. Fournier, P.F. Fischer & A. Pouquet, 2005: Geophysical-astrophysical spectral-element adaptive refinement (GASpAR): Object-oriented h -adaptive code for geophysical fluid dynamics simulation. *J. Comp. Phys.*, **submitted**.